Microstructures of bedding-parallel faults under multistage deformation: Examples from the Southeast Basin of France

N. Lemonnier, Catherine Homberg, Vincent Roche, Muriel Rocher, Anne-Marie Boullier, Johann Schnyder

Journal Pre-proof

Microstructures of bedding-parallel faults under multistage deformation: Examples from the Southeast Basin of France.

Lemonnier N, Homberg C, Roche V, Rocher M, Boullier A. M, Schnyder J

PII: S0191-8141(19)30492-4

DOI: https://doi.org/10.1016/j.jsg.2020.104138

Reference: SG 104138

To appear in: *Journal of Structural Geology*

Received Date: 22 November 2019

Revised Date: 6 July 2020

Accepted Date: 6 July 2020

Please cite this article as: N, L., C, H., V, R., M, R., M, B.A., J, S., Microstructures of bedding-parallel faults under multistage deformation: Examples from the Southeast Basin of France., *Journal of Structural Geology* (2020), doi: https://doi.org/10.1016/j.jsg.2020.104138.

Microstructures of bedding-parallel faults under multistage deformation: Examples from the Southeast Basin of France.

Lemonnier N. [1], Homberg C. [1*], Roche, V. [2], Rocher M. [3], Boullier A. M. [4], Schnyder J. [1]

1: Sorbonne Université, CNRS-INSU, Institut des Sciences de la Terre de Paris, ISTeP UMR 7193, 75005 Paris, France.
2: Fault analysis Group, UCD School of Earth Sciences, University College of Dublin, Belfield, Dublin 4, Ireland.
3: Institut de Radioprotection et de Sûreté Nucléaire, PSE-ENV/SEDRE/UEMIS, BP 17, F-92262 Fontenay-aux-Roses Cedex, France.
4: ISTerre, CNRS, Université Grenoble Alpes, F-38041 Grenoble, France.

* corresponding author

Keywords: Bedding-parallel faults, microstructures, clays, Southeast Basin of France, crack-seal veins, opening fractures.

Abstract

We conducted a microstructural analysis of bedding-parallel faults (BPFs) in Mesozoic clay-rich layers of the Southeast Basin of France. Various microstructures are recognized in thin sections under a petrographic microscope and by cathodoluminescence. The microscale observations are combined with outcrop observations from previous studies to provide insight into the origin of the BPFs and their evolution during successive phases of deformation in a basin that had a polyphase tectonic history. The BPFs have slipped while normal faults were formed during the Oligocene extension. Then, another phase of slip occurred later during the basin inversion. These two phases of deformation are expressed by recurrent crack-seal veins, pull-apart veins and stylolites. In addition, calcite veins with an elongate blocky morphology suggest an opening normal to bedding before the reactivation. The BPFs have initiated in clay layers that were shallow dipping. Such conditions may appear mechanically unfavourable for an opening normal to bedding or a shearing parallel to bedding. We suggest that the role of rock anisotropy is critical. This study furthermore demonstrates that BPFs can be long-lived brittle structures that may record successive tectonic events.

1. Introduction

Bedding-parallel faults (BPFs) are shear planes lying sub-parallel to bedding in multilayer sequences. They are usually observed in sedimentary basins in weak and compliant layers, and particularly in clay-rich layers (e.g., *Gale et al., 2014*). Typically, the shearing component is recognized through the presence of slickenlines at the outcrop scale (*Tanner, 1989; Evans, 1994; Séjourné et al., 2005; Aydin and Engelder, 2014)* and crack-seal veins at the microscopic scale *(Fowler et al., 1996; Koehn and Passchier, 2000; Fagereng and Byrnes, 2015).* The amount of displacement that is accumulated on the BPFs is usually unknown because they lie parallel to bedding, a configuration that precludes the occurrence of displaced sedimentary interfaces. Nevertheless, few studies describe BPFs offsetting other fractures which provide markers for measuring displacement (*Ferrill et al., 2000; Wibberley et al., 2007; Delogkos et al., 2017; 2018).* Based on such cross-cutting relationships, *Delogkos et al.* (*2018*) demonstrated that BPFs are segmented, display displacement gradients along their traces and die out at tips. BPFs appear therefore to have similar characteristics to other types of faults, which is why we refer to such structures as bedding-parallel faults, rather than bedding-parallel slips or bedding-parallel veins as it is commonly used in the litterature.

The presence of BPFs can influence fractures and fluid flow in basins and can be of critical importance in the frameworks of waste disposal sites, hydrocarbon reservoirs, or fluid injection operations. A variety of influences have been demonstrated. For example, BPFs can modify fault zone structures due to the process of fault restriction (*Gross et al., 1997; Roche et al., 2017*) and the removal of wall rock asperities (*Waterson et al., 1998; Delogkos et al., 2017*). BPFs can control the segmentation of hydraulic fractures and the associated microseismicity during fluid injection operations in shale (*Rutledge et al., 2015; Rutter and Mecklenburgh, 2017; Stanek and Eisner, 2017*). They can either act as a preferential fluid pathway along the beds during dilatational movement or inhibit flow across bedding due to their mineralization (*Cox et al., 1991; Cosgrove, 1993; Sibson, 1996; Rutter and Mecklenburgh, 2017*). Finally, because they often occur as a set of several planes (e.g., *Tanner, 1989; Nicol and Nathan, 2001; Delogkos et al., 2018*), BPFs can create a complex permeable mesh in the rock medium and affect permeability anisotropy.

To evaluate the impacts of bedding-parallel faults on fracturing and fluid flow throughout the history of a basin, one is required to assess their origin and their subsequent evolution during deformation history. However, this is not always straightforward because the BPFs can have various origins. They may occur, for example, with flexural-slip folding due to layer-parallel shortening or thrusting (e.g., *Tanner, 1989; Fowler, 1996, Koehn and Passchier, 2000*), in the rock volume surrounding normal faults due to fault-related folding (e.g., *Watterson et al., 1998; Ferrill et al., 2007; Smart et al., 2009*; *Delogkos et al., 2018*) and during gravity-driven deformations (e.g., *Alsop et al., 2020*).This diversity of context of formation raises critical questions concerning (i) the origin of BPFs in areas of superimposed deformation stages; (ii) the relative timing of BPFs and more steeply dipping faults; and (iii) the evolution of the BPF internal structures during deformation history.

In this paper, we describe BPFs in multilayered clay/limestone sequences from three different areas. Previous outcrop observations from the same sites have been detailed in *Roche et al. (2012a), (2012b)* and *(2017)*. Here, we focus on the microstructures of the BPFs and interpret their kinematics based on previous microscopic observations of bedding-parallel veins (e.g., *Labaume et al., 1991*; *Fowler, 1996; Koehn and Passchier, 2000; Fagereng and Byrnes, 2015)* and other veins (e.g., *Passchier and Trouw, 2005; Bons et al., 2012*). The studied areas lie in the Southeast Basin of France which has a polyphase tectonic history. By combining the microscale and the outcrop observations, we provide insight into the origin and evolution of BPFs during a complex deformation history.

2. Geological setting and methodology

2.1. Geological setting

The 40 000 km^2 Southeast Basin of France (Fig. 1) developed during Mesozoic time due to the opening of the western Tethys (or Ligurian Tethys), with up to 10 km thick sediment infill accumulated in the basin (*Dubois and Delfaud, 1989*). Extension began in the Early Triassic and lasted until the Mid Cretaceous, with a main rifting phase in Early–Mid Jurassic time, followed by several minor extensional periods (e.g., *Debrand-Passard et al., 1984; Dubois and Delfaud, 1989; Homberg et al., 2013).* Folding and thrusting occurred during the Pyrenean and Alpine orogenies, with a

paroxysm during Late Cretaceous-Eocene and Miocene times, respectively (*Ford and Stahel, 1995*). The contractional deformations were interrupted during the Upper Eocene-Oligocene by a major rifting event that developed widely in Western Europe (*Bergerat, 1987*). The Valence Graben near the studied areas (Fig. 1) is an example of a rift segment formed during this period (*Séranne, 1999*).

The BPFs have been studied in three sites, referred to as Saint-Didier, Trescléoux and Espréaux. The sites are located in the western margin (Saint-Didier) and the Vocontian trough (Trescléoux and Espréaux), a sub-basin of the Southeast Basin of France (Fig. 1). The host rocks consist of alternating clay-rich layers and limestone layers of Late Oxfordian age in Saint-Didier and Trescléoux sites and Hauterivian age in Espréaux site. The layers are shallow dipping (*ca.*10°) in Trescléoux and Saint-Didier and have been tilted in Espréaux (*ca.* 60° dipping) (Figs. 2 and 3). The BPFs are observed in the clay-rich layers and identified as thin but continuous calcite veins (millimetres thick), with a length that is limited only by the size of the outcrops (tens of meters long). The angles between the BPF and the sedimentary interfaces do not exceed a few degrees. The BPF bear slickenlines indicating a shear movement (see sub-section 2.2), but the amount of displacement has not been established due to the lack of displaced markers. The clay-rich layers hosting the BPFs are referred to below as clay layers, they are 30-200 cm thick and contain *ca.* 65% carbonate in the Late Oxfordian sequence and *ca.* 48% in the Hauterivian sequence. The limestone layers are 20-70 cm thick and contain *ca.* 80% of calcium carbonate (*Roche et al., 2014).*

2.2. Previous outcrop observations of bedding-parallel faults and other faults

In each site, other types of faults, including normal faults and strike-slip faults, are observed adjacent to the BPFs. Analyses of these structures and their interactions with the BPFs have been presented in a series of previous publications (*Roche et al., 2012a; 2012b, 2017).* Selected results of these studies that constrain the kinematics and age of the movements on the BPFs are summarized below. The normal faults that are adjacent to the BPFs strike NE-SW (Fig. 3). They predate the bed-tilting in Espréaux site and have a few centimetres to a few decimetres throw (Figs. 2 and 3). They are attributed to the Oligocene extension for two main reasons: (i) they offset Late Jurassic and Early Cretaceous sequences that post-date the major extensional Early Jurassic deformations (Fig. 1) and (ii)

the direction of the computed minimum principal stress (σ_3) responsible for the normal faulting is consistent with the extension direction during the Oligocene, i.e., WNW-ESE in Saint-Didier and Trescléoux and NW-SE in Espréaux (Figs. 1 and 3).

A set of slickenlines found on the BPFs strikes WSW-ENE in Saint-Didier and NW-SE in Trescléoux and Espréaux (Fig. 3). These directions are sub-parallel to the extension direction during the Oligocene (blue slickenlines on the stereograph of the BPFs in Fig. 3), implying that the BPFs were active at that time. Further outcrop analyses of the normal faults indicate that the BPFs acted as restrictors for the vertical propagation of the normal faults in Trescléoux and Saint-Didier (Fig. 2 a and c). This restriction is evidenced, for example, by normal faults abutting the BPF, folding of the BPF ahead of the normal fault tips, and an increase in near-tip displacement gradient with increasing maximum displacement (see *Roche et al., 2012b; 2016* for details). In Espréaux, the BPFs connect the steeper dipping normal fault segments (Fig. 2b), creating complex coherent fault zones (*Roche et al., 2012a*). Together, these observations suggest that the BPFs predated the normal faults, but that both the BPFs and the normal faults were active during the Oligocene. The burial depth at that time is unknown, but it is less than the maximum burial that occurred during the Mesozoic, i.e., 3000–6000 m at Trescléoux and Espréaux and 1600–2700 m at Saint-Didier (*Roche et al., 2016* and references therein).

The BPF bear a second set of slickenlines in Espréaux and Trescléoux (red slickenlines on the stereograph of the BPFs in Fig. 3) that is oblique to the Oligocene extension direction described above, i.e., NE-SW in Espréaux and NNE-SSW in Trescléoux. In Espréaux, this direction is slightly oblique to the fold hinge trend (N170) and compatible with the ENE-WSW orientation of the Alpine compression inferred from strike-slip faults in this site, taking into account the tilting of the fold hinge (Fig. 3b). In Trescléoux, the NNE-SSW slickenlines on the BPF are parallel to the compression direction deduced from strike-slip faults that may have occurred either during the Pyrenean or Alpine phases, considering the regional stress calendar (Fig. 1). In Saint-Didier, no reactivation of the BPF and no strike-slip faults are observed at the outcrop scale.

2.3. Microscopic analysis

Oriented rock samples were collected in each of the studied sites for prepararing thin sections (Tab. 1 and Fig. 2). The clay layers can be subject to severe surface alterations and pristine samples were drilled at a depth of 10-20 cm with a 5 cm and 2.5 cm plug. Drilling frequently resulted in destroying the samples and the procedure was repeated several times to recover samples of a suitable size for the thin section preparation. In Espréaux, 4 different BPFs were targeted, but only 12 thin sections from 2 BPFs were successfully retrieved (Tab. 1). In Trescléoux and Saint-Didier respectively, 7 and 3 thin sections of a unique BPF were retrieved (Tab. 1). All the thin sections are cut perpendicular to the BPF planes and parallel to the average directions of the extension-related striation. Each thin section was observed under a petrographic microscope in optics. Selected areas were further investigated with CL images obtained with a cold cathode of type Cathodyne-OPEA, 15–20 kV and 200 to 400 µA mm^2 under a pressure of 0.05 Torr. A numerical Nikon D70 (800 ASA) camera was used for the acquisition of the luminescence images.

3. Description of microstructures

The BPFs show a laminated aspect at the microscale, with stacked and millimetres thick sub-parallel sheets of calcite separated by wall-rock slices (Fig. 4). In the following sub-sections we combine observations from the different sites and present the main microstructures of the BPFs that have been observed recurrently in the different thin sections (Tab. 1).

3.1. Bedding-parallel calcite veins and satellite veins

In the three sites the BPFs consist of bedding-parallel mineralized veins which are tens of millimetres thick and continuous across the thin sections. These veins are filled with calcite crystals and are referred to below as calcite veins (e.g., (C.V.) in Fig. 4). Their infilling consists of large crystals with a blocky to elongate blocky morphology (Figs. 4 and 5a). The elongate crystals are several micrometres to millimetres long and orthogonal to the edges of the veins (syntaxial vein, see *Bons et al., 2012*). In all sites, most crystals are twinned and contain many solid inclusions giving them a characteristic “dirty” aspect (Fig. 4). The calcite crystals, the traces of solid inclusions and the clays in the wall rocks have a similar dark orange colour in CL images, indicating an equilibrium

between the host rock and the veins (Fig. 6). In Saint-Didier and Espréaux, the veins are sealed by the elongate crystals, whereas cavities are observed between the crystals in Trescléoux (e.g., (Cav.) in Fig. 4c). The cavities are elongate and partly filled with successive layers of crystal that display internal zoning. The first layer from the elongate crystals consists of very thin, concentric and untwinned "clean" calcite crystals, appearing orange with alternative brightness in CL images (Fig. 6d). This alternation is interpreted as an overgrowth, with interruption of the fluid flow marked by toothless, dissolved crystals. The second layer corresponds to an iron oxide filling that appears yellow in plane polarized light. Finally, the last layer before open cavities is made of fibrous crystals that are not luminescent in CL (Fig. 6d). In addition to the calcite veins described above, narrow veins, referred to as satellite veins, have also been observed (e.g., (S.V.) in Fig. 4). In Espréaux, these veins are composed of small or large calcite crystals that are fibrous with fibres that are perpendicular to the vein margins, and thus to bedding (e.g., Fig. 4e).

3.2. Crack-seal veins and pull-apart veins

In the three studied sites the BPFs also consist of a series of successive, *en échelon*, mineralized veinlets that are separated by thin wall-rock slices (e.g., (C.S.) in Fig.4). These structures are interpreted to result from a crack-seal mechanism. Accordingly, the veinlets are considered as opening fractures that formed between overstepping shear planes (microfaults) and due to periodic fracturing and sealing during slip increments (e.g., *Ramsay, 1980; Gaviglio, 1986; Labaume et al., 1991; Fowler, 1996*; *Renard et al., 2005*). The array of successive veinlets and wall-rock slices (crack-seal bands) together compose a vein, referred to as a crack-seal vein, that is parallel to bedding. The microfaults bounding the crack-seal veins are also parallel to bedding implying a bedding-parallel shear. In Espréaux several crack-seal veins that are millimetres thick are juxtaposed on top of each other (Figs. 4e and 5d). The individual veinlets within the crack-seal veins are closely spaced and dip to the west at a mean 35° to 60° angle to bedding. Some veinlets are curved, which may be due to deflected stresses and/or rotations produced by the shear movement. In Trescléoux, the crack-seal veins are typically located at the edge of the calcite veins and are bound by slip surfaces that are not well-preserved ((C.S.) in Figs. 4c and 6c). The veinlets are observed between well-develloped wall

rock slices, are more spaced than in Espréaux, appear sinuous, and dip at 45° to bedding. In Saint-Didier, the crack-seal veins are thinner (infra-millimetric). The veinlets have a shallower dip and are filled with calcite crystals (<50µm) with a blocky texture ((C.S.) in Figs. 4a and 6a).

Slip along the BPFs is further demonstrated in Espréaux by mineralized pull-apart veins of various sizes (up to a centimetre long) that display a lozenge shape (rhomboid) (e.g., Figs. 5e and 6f). These pull-apart veins sometimes superpose on top of each other forming a composite pull-apart vein (e.g., Figs. 5e and 6f). The crystals within these veins are often elongated in the direction parallel to the BPF, the vein walls are west-dipping (e.g., Fig. 6f) and crack-seal morphologies are sometimes present on the vein walls (Fig. 5e). These pull-apart veins are interpreted as having formed in extensional stepovers between microfault segments (e.g., *Peacock et al., 1995*). The opening direction is sub-parallel to bedding and the shear sense is similar to that responsible of the crack-seal veins described above.

3.3. Breccia

In Saint-Didier, the BPF appears locally as a zone of breccia ((Br.) in Fig.4 a and b). Calcite crystals of the calcite veins are sometimes preserved on the rim of the BPF, whereas the BPF is filled with microbreccia in the centre. The microbreccia is made up of angular clasts of calcite and wall-rock fragments (less than a few mm) floating within a clay matrix (Fig. 4 a and b). CL analysis shows that the calcite crystals in the microbreccia have a brighter orange colour than the calcite crystals in the calcite veins (Fig. 6b), indicating the presence of new fluid. The breccia also contains broken crystals (0.25 mm) from the former calcite veins. No breccia are observed in Trescléoux and Espréaux thin sections, but we recognize zones of significant shearing in Espréaux. These zones are described in the next sub-section.

3.4. Stylolites and other calcite-filled features

In the three sites, the calcite veins, satellite veins, crack-seal veins, and pull-apart veins are most often separated from each other or from the hosting clays by well defined straight surfaces. However, some veins are bounded by stylolite planes that occur at the clay/calcite boundary ((St.) in

Fig. 4). Such planes are also observed within the calcite veins. Like the calcite veins, the stylolites are sub-parallel to BPF. The amount of dissolution associated with these stylolites is difficult to estimate and may be significant. Stylolite planes appear more frequently in Espréaux and Saint-Didier than in Trescléoux, which may indicate that pressure solution is more pronounced in these sites.

Other mineralized structures are observed in Espréaux (Fig. 7). Despite the uncertainty in their interpretation, two microstructures that suggest shearing are worth mentioning. The first one corresponds to rectangular and discontinuous veins filled with large crystals (Fig. 7 a and b). These angular structures are interpreted as broken fragments of the calcite veins which have been toggled and rotated within a clay-rich matrix. Finally, small dimension (tens of micrometres) and mineralized structures with fuzzy boundaries are observed ((F. V.) in Figs. 7e and f). These structures seem to have an *en échelon* arrangement, which can be used as a shear sense indicator. The kinematics of these structures are discussed further in sub-section 4.3.

4. Microstructures interpretations and kinematics

4.1. Saint-Didier

The microstructures described in Section 3 suggest that different movements occurred along the BPF plane (Tab. 1). The calcite veins with elongate-blocky crystals are interpreted as syntaxial veins, with an opening direction normal to bedding (*Bons et al., 2012*). CL images show that the solid inclusions observed within the calcite veins are fragments of the wall rock and that the fluid that filled the BPFs and the hosting rock were in equilibrium. The crack-seal veins indicate a shear opening (*Cox et al., 1983; Cox, 1987; Labaume et al., 1991; Koehn and Passchier, 2000*). They are parallel to bedding with internal veinlets that are westward dipping, suggesting a movement parallel to bedding and with a top-to-the-west shear sense. The normal faults are mostly dipping west and also have a top-to-the-west movement (Figs. 2 and 3). The BPF and the normal faults have therefore a synthetic movement. We have not found any direct microscopic evidence to constrain the chronology between opening and shearing, but CL images indicate that the fluids that circulated during these two events were in equilibrium. The stylolites are sub-parallel to the BPF. They affect the calcite veins and

therefore the dissolution postdated the opening. Finally, the microbreccia is composed of clasts from the calcite veins and is associated with a different fluid. These observations suggest that the microbreccia also postdated both the opening and shearing event. This microbreccia is thought to result from seismic cataclastic events (*Boullier et al., 2004*), but the absence of markers prevents determining the shear sense.

4.2. Trescléoux

The microstructures observed in Trescléoux suggest opening, shearing and pressure solution, like in Saint-Didier site (Tab. 1). The elongate-blocky morphology of the crystals in the calcite veins suggest an opening normal to the BPF, i.e., an opening subperpendicular to bedding. The geometry of the crack-seal veins and associated veinlets indicates a movement parallel to bedding and top-to-the-west, which is synthetic to the movement of the normal faults. The crack-seal veins are located at the edges of the calcite veins. According to the CL images, the crystals in the calcite veins and the crack-seal veins were derived from the same fluid that is in equilibrium with the hosting rock (Fig. 6). Stylolitisation of the calcite veins and probably of the crack seal veins indicate a dissolution at high angle to bedding that appears to be the last phase of deformation. Further crystallisations are observed around cavities within the calcite veins. Crystal zoning by optic and catodoluminescence and crystallisations that isopachously follow the irregularities of the cavity walls are indicative of growth into cavities. The CL images indicate that these crystals were derived from another fluid during an across-strata or larger scale fluid circulation.

4.3. Espréaux

The calcite veins, crack-seal veins and stylolites indicate opening, shearing and stylolitization along the BPFs, like for the two other sites (Tab. 1). Crystals in the calcite veins are occasionally elongate with a direction of maximum extension perpendicular to the BPFs, implying an opening perpendicular to bedding. This opening direction is confirmed by the fibrous morphology of the crystals in the satellite veins, considering that the fibres that are oriented normal to bedding follow the

opening trajectory. The geometry of the crack-seal veins indicates a movement parallel to bedding with a top-to-the-west shear sense. This shear sense is further confirmed by the pull-apart veins that have west-dipping walls. Contrary to the other sites, this movement is not synthetic to that of the normal faults, implying that it does not originate from the same phase of extension but from another tectonic event (see sub-section 5.1). The CL images indicate that the sealing of the pull-apart veins, the calcite veins and the crack-seals veins were derived from a fluid in equilibrium with the host rock.

The kinematics of the small dimension mineralized structures (Fig. 7f) are difficult to characterize due to their fuzzy aspect. We recognized an *en échelon* pattern with an east-dipping trend. We tentatively infer a top-to-the-east shear movement, with development of T or R Riedel fractures. These fractures may attest for a first movement synthetic to that of the normal faults. Later sliding in the opposite direction then stretched these fractures. Finally, the rectangular mineralized elements are interpreted as broken segments of the calcite veins forming imbricated structures in clay due to a top-to-the-west shear movement (Fig.7c). This movement postdates the opening event and is in agreement with the sliding episode that produced the sub-parallel sets of *en échelon* crack-seal bands in this site. Alternatively, the observed arrangement may result from a clockwise rotation of the broken pieces of the calcite veins during a shear movement synthetic to that of the normal faults (Fig. 7d).

5. Discussion

The microstructures of the bedding-parallel faults (BPFs) observed in clay-rich layers of the Southeast Basin of France, reflect a complex deformation history with a range of movements that includes bedding-normal opening, bedding-parallel shearing and pressure solution. In the next sub-sections, we combine the microstructural information with the outcrop observations to discuss the possible origins, mechanisms of formation and geological settings of BPFs in general.

5.1. BPFs and regional tectonic history

Bedding-parallel shear movements are associated with crack-seal bands on the studied BPFs, which is consistent with previous observations in other areas (*Fowler, 1996; Koehn and Passchier, 2000; Fagereng and Byrnes, 2015*). The orientations of the slikenlines on the BPFs indicate that the

shear movements likely occurred during the Oligocene extension and the Pyrenean and/or Alpine orogenies (Figs. 1 and 2). The BPFs also contain calcite veins with elongate blocky textures and fibrous crystals, which are interpreted to be produced by bedding-parallel openings (*Bons et. al, 2012*). Finally, bedding-parallel stylolites are recognized in the three studied sites, implying pressure solutions. The stylolites postdate the opening of the calcite veins and probably also the crack-seal veins. Breccia, "broken veins" and imbricate structures are also observed in a few thin sections and these could be associated with an increase in the magnitude of the shear movements and/or in the fluid pressure.

The absolute age of the microstructures are prone to uncertainties but the relative chronologies described above help to constrain potential models of formation and evolution of BPFs in the geological context of the Southeast Basin of France (Fig. 8). The different models presented in Figure 8 are intended to provide insight into the range of potential movements and associated microstructures of BPFs during a polyphase deformation history in general. The mechanical conditions required for these models are discussed further in sub-section 5.2.

In Model 1, all the microstructures are formed during the Oligocene, i.e., monophase deformation (Fig. 8). Calcite veins and crack-seal veins can be due to a succession of alternating opening and shearing, which can potentially be associated with a "crack-seal/slip" model (*Petit et al., 1999*). Stylolites can then dissolve the calcite veins with an orientation that is compatible with the vertical direction of the maximum principal stress. While this scenario can eventually apply in Saint-Didier site where there is no evidence of reactivation, it is unlikely in Espréaux and Trescléoux where the BPFs bear slikenlines with two radically distinct orientations.

In the two other models presented in Figure 8, the BPFs result from a polyphase deformation. In Model 3, the calcite veins have formed before the Oligocene extension and the associated normal faults. They may have opened due to fluid overpressures, which have hydraulically jacked apart near-horizontal bedding planes during the Mesozoic burial history. Altenatively, they may have formed as tectonic fractures opening perpendicularly to the maximal principal stress direction during the Pyrenean orogeny. In Model 2, the calcite veins formed during the Alpine orogeny. Thus, depending

on the age of the calcite veins, the BPFs either have initiated as shear planes in low dipping sequences during the Oligocene extension (Model 2) or have reactivated previous opening structures (Model 3). In addition, three possible origins can be proposed for the stylolites, based on models which have been described in the literature (*Nitecki, 1962*, *Toussaint et al., 2018)*. They may have originated (1) as sedimentary stylolites during the Mezosoic burial history, (2) as tectonic stylolite planes oriented perpendicularly to the direction of maximal principal stress during the Oligocene extension, and (3) as slickolites in restraining steps due to the slips on the BPFs. In Model 2, the opening occurred late in the BPF history, the stylolites that postdate the opening have therefore a tectonic nature (origin 3). By contrast, if the opening occurred early, then the three origins described above (origins 1-3) may apply in the studied sites (Model 3).

The models in Figure 8 illustrate that BPFs can be polyphase structures that are active during successive deformational events. This concurs with the findings of *Séjourné et al. (2005*) that describe five different senses of slip motion on a series of BPFs in the Saint-Dominique carbonate slice (southern Quebec Appalachian structural front), which are consistent with folding, thrusting, strike-slip faulting and normal faulting. The existence of long-lived BPFs has the following implications: (1) BPFs can be used as a marker of past deformation events to reconstruct complex deformation history, (2) BPFs can appear as relatively simple planes at the macroscale, despite a complex deformation history, and (3) BPFs can be considered as a plane of weakness in the geological medium.

5.2. Mechanical insight into bedding-parallel faulting in sedimentary rocks

Microstructural and outcrop observations indicate that shearing (and eventually opening) occurred along the BPFs during normal faulting and before folding. This is in line with the results of recent publications that describe BPFs associated with normal faults in shallow dipping sequences (<10°; *Delogkos et al., 2017; Alsop et al., 2020*). Shearing in such conditions appear mechanically unfavourable and can be related to several driven mechanisms. First, the mechanical anisotropy of the clay-rich rocks can promote failure and slip, even if the foliation is not optimally oriented (*Cobbold et*

al., 2013; Fagereng et al., 2010). Second, even at low magnitudes, a local tilting of the bedding could enhance shearing along the foliation. Finally, fluid pressure may have a role, but the BPFs in the studied areas have a relatively small thickness (mm thick), which may suggest a limited pore pressure. Concerning the opening of the BPFs, it is expected to occur under low differential stress. Such conditons are generally encountered at low depth, but also exist at a more significant depth in clay rich rocks with a very low stiffness (*Warpinski and Teufel, 1991*) or in relations with ductile flow in the clay (*Cornet and Röckel, 2012*)

There is a widespread occurrence of crack-seal veins associated with shear opening on the studied BPFs and on BPFs from other areas (*Fowler, 1996; Koehn and Passchier, 2000; Fagereng and Byrnes, 2015*). Considering that these crack-seals are formed in extensional stepovers, this suggests that the BPFs are segmented by nature, independently of their origin. Moreover, the crack-seal veins indicate that the displacement is accommodated by small increments. The slippage is therefore expected to be associated with a seismic activity of low magnitude (*Fagereng et al., 2010).* Nevertheless, more significant seismic activities could potentially occur and be marked by microstructures like breccia and imbricate structures as those observed in the studied sites.

The repeated activity of the BPFs during successive tectonic phases lead us to consider these structures as planes of weakness in the geological medium. However, the calcite mineralizations that filled the BPFs are probably “stronger” than the surrounding clays. This inconsistency demonstrates that the process of reactivation is not necessarily associated with intrinsically weak planes. On the contrary, we propose that reactivation is promoted at boundaries between materials of different nature or inherited mechanical heterogeneities, i.e., the vein/clay edges in this study. A similar process occurs for dyke walls that are often the locus of faulting in volcanic areas (e.g., *Karson et al., 2018*). It is also in agreement with the idea that preferential growth of fault is not positively correlated with the intrinsic weakness properties of faults (*Walsh et al., 2001*). This process of ‘forced slip’ is likely driven by stress concentrations that occur in heterogeneous medium (e.g., *Gudmundsson and Homberg, 1999; Gunzberger and Cornet, 2007*), but the geological conditions where forced slip may control the fault pattern and slip accumulation through time are still to be investigated.

5.3. Driving mechanisms behind BPF formation at the regional scale

The studied BPFs show shear movement during an extensional regime in all the studied sites, as well as shear movement during a compressional regime in two of the studied sites. The compression related-slip can be attributed to a flexural slip mechanism during layer-parallel folding (e.g., *Tanner, 1989; Fowler, 1996; Koehn and Passchier, 2000; Fagereng et al., 2010*). However, while flexural slip can be important in Espréaux where the BPF lie on the limb of a tight fold, it is likely less important in Trescléoux where the bedding is sub-horizontal.

The shear movements during the extensional regime confirm other publications showing that BPFs may form in such context for a limited local tilting of the bedding (<10°) (*Smart et al., 2009; Delogkos et al., 2018; Alsop et al., 2020*). The movements on the BPFs could be attributed to a flexural slip mechanism due to normal fault-related folding (*Watterson et al., 1998; Ferrill et al., 2007; Smart et al., 2009; Delogkos et al., 2018*) or to gravity-driven downslope deformations (e.g., *Alsop et al., 2020*). The latter is unlikely in the studied areas, considering that the rocks have been deeply buried before the formation of the BPF. More generally, the exact origin of the extension-related bedding-parallel shearing remains uncertain. Two models can nevertheless be proposed, which are differing in how the BPFs and the normal faults relate. In the first model (Fig. 9a), the mesoscale normal faults are formed to accommodate the motions between overstepping BPFs. Equivalent geometries, referred to as "ramp-flat-ramp normal faults" and releasing relay zones, have been described previously by *Pedrera et al. (2012)* in alternating sandy and silt layers of the Huércal-Overa Basin and by *Delogkos et al. (2018)* in intercalated lignites and alluvial deposits of the Ptolemais Basin, respectively. The orientation and displacement of the normal faults are hereby governed by the BPF motion. Alternatively, the BPFs and the normal faults can be formed independently and express different modes of brittle failure in multilayer materials (Fig. 9b). Considering the large angle between the far-field maximum principal stress and the BPF in an extensional regime, a failure along a BPF in clay units does not fit the Anderson model, whilst it does along a high dipping normal fault. We refer to this as "bi-modal" faulting, which can be a characteristic mode of deformation of anisotropic rocks. "Bi-modal" faulting is likely to develop in multilayer sequences containing isotropic and anisotropic

rocks, but its origin need to be investigated. In the two models, BPFs and normal faults may strongly interact at some evolved stages.

Conclusions

The microstructural descriptions of bedding-parallel faults (BPFs) sampled in clay-rich layers of the Southeast Basin of France evidenced that these faults are composed of different microstructures. These microstructures include subparallel calcite veins, crack-seal veins, pull-appart veins, microfaults, stylolites and breccia. Both opening and shearing that are perpendicular and parallel to bedding, respectively result in fluid channelling in the BPFs through repeated crack and seal events. The observations support a complex deformation history of BPFs. Sliding occurred under an extensional stress regime during the Oligocene and the BPFs strongly interacted with surrounding normal faults. The BPFs were also reactivated in an opposite sense during the basin inversion. This study highlights that BPFs are relevant markers of past deformation events to reconstruct complex deformation history. They can represent well developed brittle structures in shallow or highly dipping foliated rocks and influence the growth of other fractures.

Acknowledgements

The authors thank M. De Rafaelis for the help on cathodoluminescence and IRSN who sponsored this study. Paul Bons and an anonymous reviewer, together with editor Ian Alsop, are thanked for their constructive reviews and comments, which enhanced the quality of this manuscript.

References

Alsop, G., L., Weinberger, R., Marco, S., Levi, T., 2020. Bed-parallel slip: Identifying missing displacement in mass transport deposits. Journal of Structural Geology 70, 103952.

445 Angelier, J., 1984. Tectonic analysis of fault slip data sets. Journal of Geophysical Research: Solid
446 Earth 89, 5835-5848. Koehn, D., Passchier, C., W., 2000. Shear sense indicators in striped
447 bedding-veins. Journal of Structural Geology 22, 1141-1151.
448 Aydin, M. G., Engelder, T., 2014. Revisiting the Hubbert–Rubey pore pressure model for overthrust
449 faulting: Inferences from bedding-parallel detachment surfaces within Middle Devonian gas shale,
450 the Appalachian Basin, USA. Journal of Structural Geology 69, 519-537.
451 Bons, P.D., Elburg, M.A, Gomez-Rivas, E., 2012. A review of the formation of tectonic veins and
452 their microstructures. Journal of Structural Geology 43, 33-62.
453 Boullier A.-M., Fujimoto K., Ohtani T., Roman-Ross G., Lewin E., Ito H., Pezard P., Ildefonse B,
454 2004). Textural evidence for recent co-seismic circulation of fluids in the Nojima fault zone, Awaji
455 island, Japan Tectonophysics 378, 165– 181.
456 Cobbold, P.R., Zanella, A., Rodrigues, N., Løseth, H., 2013. Bedding-parallel fibrous veins (beef and
457 cone-in-cone): Worldwide occurrence and possible significance in terms of fluid overpressure,
458 hydrocarbon generation and mineralization. Marine and Petroleum Geology 43, 1-20.
459 Cornet, F. H., & Röckel, T., 2012. Vertical stress profiles and the significance of “stress decoupling”.
460 Tectonophysics 581, 193-205.
461 Cosgrove, J.W., 1993. The interplay between fluids, folds and thrusts during the deformation of a
462 sedimentary succession. Journal of Structural Geology 15, 491-500.
463 Cox, S.F., 1987. Antitaxial crack-seals vein microstructures and their relationship to displacement
464 paths. Journal of Structural Geology 9, 779-787.
465 Cox, S.F., Etheridge, M.A., 1983. Crack-seals fibre growth mechanism and their significance in the
466 development of oriented layer silicate microstructures. Journal of Structural Geology 92, 147-170.
467 Cox, S.F., Wall, V.J., Etheridge, M.A., Potter, T. F., 1991. Deformational and metamorphic processes
468 in the formation of mesothermal vein-hosted gold deposits—examples from the Lachlan Fold Belt
469 in central Victoria, Australia. Ore geology reviews 6, 391-423.
470 Debrand-Passard, S., Courboulaix, S., Lienhardt, M.- J., 1984. Synthèse géologique du Sud-Est de la
471 France, Mém. BRGM, France 125, 1, 614 p.

Delogkos, E., Childs, C., Manzocchi, T., Walsh, J.J., Pavlides, S., 2017. The role of bed-parallel slip in the development of complex normal fault zones. Journal of Structural Geology 97, 199-211.

Delogkos, E., Childs, C., Manzocchi, T., Walsh, J.J., 2018. The nature and origin of bed-parallel slip in Kardia Mine, Ptolemais Basin, Greece. Journal of Structural Geology 113, 115-133.

Dubois, P., Delfaud, J., 1989. Le bassin du Sud-Est. In: Dynamique et méthodes d'étude des bassins sédimentaires. Association des Sédimentologistes français, Ed. Technip, Paris, France, 277-296.

Evans, M.A., 1994. Joint and decollement zones in Middle Devonian shales: Evidence for multiple deformation events in the central Appalachian Plateau. Geological Society of America Bulletin106, 447-460.

Fagereng, Å., Remitti, F., Sibson, R.H., 2010. Shear veins observed within anisotropic fabric at high angles to the maximum compressive stress. Nature Geoscience 3, 482.

Fagereng, A., Byrnes, G., 2015. A range of fault slip styles on progressively misoriented planes during flexural-slip folding, Cape Fold Belt, South Africa. Journal of Structural Geology 70, 156-169.

Ferrill, D.A., Morris, A.P., Stamatakos, J.A., Sims, D.W., 2000. Crossing conjugate normal faults. AAPG bulletin 84, 1543-1559.

Ferrill, D.A., Morris, A.P., Smart, K.J., 2007. Stratigraphic control on extensional fault propagation folding: Big Brushy Canyon monocline, Sierra del Carmen, Texas. Geological Society, London, Special Publications, 292, 203-217.

Fowler, T., J., 1996. Flexural-slip generated bedding-parallel veins from central Victoria, Australia. Journal of Structural Geology 18, 1399–1415.

Gale, J.F., Laubach, S.E., Olson, J.E., Eichhubl,P., Fall, A., 2014. Natural fractures in shale: A review and new observations Natural Fractures in Shale: A Review and New Observations. AAPG bulletin, 98, 2165-2216.

Gaviglio, P., 1986. Crack-seal mechanism in a limestone: A factor of deformation in strike-slip faulting. Tectonophysics 131, 247-255.

Gross, M.R., Gutiérrez-Alonso, G., Bai, T., Wacker, M.A., Collinsworth, K.B., Behl, R.J., 1997. Influence of mechanical stratigraphy and kinematics on fault scaling relations. Journal of Structural Geology 19, 171-183.

Gudmundsson, A., Homberg, C., 1999. Evolution of stress fields and faulting in seismic zones, Pure and applied geophysics 154, 257-280.

Gunzburger, Y.; Cornet, F. H., 2007. Rheological characterization of a sedimentary formation from a stress profile inversion. Geophysical Journal International 168, 402-418.

Homberg, C., Schnyder, J., Benzaggagh, M., 2013. Late Jurassic-Early Cretaceous faulting in the Southeastern French Basin: does it reflect a tectonic reorganization? Bulletin de la Société Géologique de France 184, 501-514.

Jessell, M.W., Willman, C.E., Gray, D.R., 1994. Bedding parallel veins and their relationship to folding. Journal of Structural Geology 16, 753- 767.

Karson, J.A., Farrell, J.A., Chutas, L.A., Nanfito, A.F., Proett, J.A., Runnals, K.T., Sæmundsson, K., 2018. Rift-parallel strike-slip faulting near the Iceland plate boundary zone: Implications for propagating rifts. Tectonics 37, 4567–4594.

Labaume P., Berty C., Laurent P., 1991. Syn-diagenetic evolution of shear structures in superficial nappes: an example from the Northern Apennines (NW Italy). Journal of Structural Geology 13, 385-398.

Nicol, A., Nathan, S., 2001. Folding and the formation of bedding-parallel faults on the western limb of Grey Valley Syncline near Blackball, New Zealand. New Zealand. Journal of Geology and Geophysics 44, 127-135.

Nitecki, M.H., 1962. Observations on slickolites. Journal of Sedimentary Research, 32, 435-439.

Passchier, C.W., Trouw, R. A. J., 2005. Microtectonics, second ed. Springer-Verlag,Berlin/Heidelberg.http://dx.doi.org/10.1007/3-540-29359-0.

Pedrera, A., Galindo-Zaldívar, J., Lamas, F., Ruiz-Constán, A., 2012. Evolution of near-surface ramp-flat-ramp normal faults and implication during intramontane basin formation in the eastern Betic Cordillera (the Huércal-Overa Basin, SE Spain). Tectonics 31, doi:10.1029/2012TC003130.

Petit, J.P., Wibberley, C.A., Ruiz, G., 1999. Crack–seal', slip: a new fault valve mechanism? Journal of Structural Geology 21, 1199-1207.

Ramsay, J.G., 1980. The crack-seals mechanism of rock deformation. Journal of Nature 284.

Renard, F., Andréani, M., Boullier, A.M., Labaume, P., 2005. Uncorrelated stress release variations in crustal rocks. In: Geological Society, London, Special Publications 243. 67-79.

Roche, V., Homberg, C., Rocher, M., 2012a. Fault displacement profiles in multilayer systems: from fault restriction to fault propagation. Terra Nova 24, 499-504.

Roche, V., Homberg, C., Rocher, M., 2012b. Architecture and growth of normal fault zones in multilayer systems: a 3D field analysis in the South-Eastern Basin, France. Journal of Structural Geology 37, 19-35.

Roche, V., Homberg, C., David, C., Rocher, M., 2014. Normal faults, layering and elastic properties of rocks. Tectonophysics 622, 96-109.

Roche, V., Homberg, C., van der Baan, M., Rocher, M., 2017. Widening of normal fault zones due to the inhibition of vertical propagation. Geological Society, London, Special Publications 439, 271-288.

Rutledge, J., Yu, X., Leaney, S., 2015. Microseismic shearing driven by hydraulic-fracture opening: An interpretation of source-mechanism trends. The Leading Edge 34 926-934.

Rutter, E. H., Mecklenburgh, J., 2017. Hydraulic conductivity of bedding-parallel cracks in shale as a function of shear and normal stress. Geological Society, London, Special Publications 454, 67-84.

Séjourné, S., Malo, M., Savard, M. M., Kirkwood, D., 2005. Multiple origin and regional significance of bedding parallel veins in a fold and thrust belt: the example of a carbonate slice along the Appalachian structural front. Tectonophysics 407, 189-209.

Seranne, M., 1999. The Gulf of Lion continental margin (NW Mediterranean) revisited by IBS: an overview. SERANNE, M. 1999. The Gulf of Lion continental margin (NW Mediterranean) revisited by IBS: An overview. In: Durand, B., Jolivet, L., Horváth, E., Seranne, M., (eds) The Mediterranean Basins: Tertiary Extension within the Alpine Orogen. Geological Society, London, Special Publications 156, 15-36.

Sibson, R. H., 1996. Structural permeability of fluid-driven fault-fracture meshes. Journal of Structural Geology 18, 1031-1042.

Smart, K.J., Ferrill, D.A., Morris, A P., 2009. Impact of interlayer slip on fracture prediction from geomechanical models of fault-related folds. AAPG bulletin 93, 1447-1458.

555 Staněk, F., Eisner, L., 2017. Seismicity induced by hydraulic fracturing in shales: A bedding plane slip
556 model. Journal of Geophysical Research, Solid Earth 122, 7912-7926.
557 Tanner, P. G., 1989. The flexural-slip mechanism. Journal of Structural Geology 11, 635-655.
558 Walsh, J. J., Childs, C., Meyer, V., Manzocchi, T., Imber, J., Nicol, A., ... Nell, P. A., 2001. Geometric
559 controls on the evolution of normal fault systems. Geological Society, London, Special
560 Publications 186, 157-170.
561 Warpinski, N. R., & Teufel, L. W., 1991. In situ stress measurements at Rainier Mesa, Nevada test
562 site—influence of topography and lithology on the stress state in tuff. In International Journal of
563 Rock Mechanics and Mining Sciences & Geomechanics Abstracts 28, 143-161.
564 Watterson, J., Childs, C., Walsh, J.J., 1998. Widening of fault zones by erosion of asperities formed by
565 bed-parallel slip. Geology 26, 71-74.
566 Wibberley, C.A.J., Petit, J.P., Rives, T., 2007. The effect of tilting on fault propagation and network
567 development in sandstone - Shale sequences: A case study from the Lodève Basin, southern
568 France. Journal of the Geological Society 164, 599-608.
569

		Saint-Didier	Trescléoux	Espréaux
BPF Samples				
Number of distinct BPFs		1	1	2
Number of thin sections		3	7	12
Types of microstructures	**Kinematics**	**Number of thin sections**		
Calcite veins	Opening [(1)]	3	7	12
Crack-seal veins	Shearing [(2)]	1 SNF	1, SNF	2, ANF
Pull-aparts veins	Shearing [(2)]			1 ANF
Breccia	Intense shearing[(2)]	3, US		
Broken veins	Intense shearing[(2)]			1, US
Fuzzy structures	Shearing?			1, SNF
Stylolitized planes	Dissolution	1	5	6

Tab. 1: Type and interpretation of microstructures observed in thin sections.

Four bedding-parallel faults (BPFs) were targeted in Espréaux, only two of them were successfully retrieved. The numbers of thin sections showing each microstructure type is indicated in column for each site. (1): Opening indicates an opening movement perpendicular to the BPF. (2): SNF and ANF denote shearing (i.e., sliding) with a shear sense that is synthetic (SNF) or antithetic (ANF) with the neighboring normal faults, i.e., movement in the same oropposite direction as that of the hanging wall movement of the normal faults, respectively. US: shearing with unknown sense.

Fig. 1: Simplified geological map of the North West region of the Southeast Basin of France (modified from *Roche et al. (2014)*) and tectonic calendar of the basin. Tectonic events are based on analyses from *Constantin et al. (2012)*, *Lamarche et al. (2012)*, *Homberg et al. (2013)* and references therein. Light grey and dark grey indicate extensional and compressive deformation phases, respectively. The ages of the formations hosting the bedding-parallel faults (BPFs) are indicated by a black arrow. The BPFs are located in Saint-Didier, Trescléoux and Espréaux sites.

Fig. 2: Context of bedding-parallel faults (BPFs) and sampling in Trescléoux (a), Espréaux (b) and Saint-Didier (c). Normal faults (NF), offsetting the limestone and clay layers, and the bedding-parallel faults (BPFs) are indicated. The limestone and clay layers are represented in light and dark grey, respectively. The numbering indicates the location of the BPF sampling for the thin sections. Examples of details of sampling are presented in the right panel.

Fig. 3: Stereographic projections (lower-hemisphere, equal-area projection) for the Saint-Didier site (a), the Trescléoux site (b) and the Espréaux site (c). Data for the bedding-parallel faults (BPFs), the normal faults and the strike-slip faults are back-tilted using the average tilting of the bedding. Solid circles: fracture planes. Small black dots and arows: slickenlines. n: the number of data. Stars with 5, 4, 3 branches: maximal (σ_1), intermediate(σ_2), and minimal (σ_3) principal stress. Divergent and convergent arrows: directions of the extension (σ_3) and compression (σ_1). Small blue and red dots: slikenlines on the BPFs that are coherent with the direction of extension (blue) and the direction of compression (red) found using the normal faults and the strike slip faults, respectively.

Fig. 4: Thin sections of bedding-parallel faults (BPFs). (a) and (b): Saint-Didier; (c): Trescléoux; (d) and (e): Espréaux. (a-e). Different microstructures are observed. C.V.: Calcite vein; Cl.: Clays (wall rock); C.S.: Crack-seal vein; S.V.: Satellite vein; St.: Stylolite; Br.: Breccia; Cav.: Cavity. Location of details illustrated in Figures 5 and 6. So: Bedding.

Fig. 5: Details of microstructures within bedding-parallel faults (BPFs). (a) Elongate blocky crystal morphology in Saint Didier. (b) Shallow dipping veinlets in crack-seal veins indicating a top-to-the-west movement in Saint Didier. West is to the right. (c) Stylolite in calcite veins in Espréaux in optics and cathodoluminescence. (d) Supperposed crack-seal veins in Espréaux. (e) Pull-appart veins in Espréaux. (a-e) C.V.: Calcite vein; Cl.: Clays (wall rock); C.S.: Crack-seal vein; S.V.: Satellite vein; St.: Stylolite. So: Bedding.

Fig. 6: Details of the microstructures in transmitted light and cathodoluminescence. (a) and (b): Saint Didier (c-e): Trescléoux; (f) and (g): Espréaux. (a) Bedding veins and clays in wall rock display a dark orange colour. (b) Breccia with a brighter orange than the calcite forming initially the BPF, indicating different fluid generations. (c) Caclite vein and crack-seal veins. (d) Cavities infiling with various

fluids. (e) Calcite veins and stylolites. (g) Pull-apart veins. (a-f) C.V.: Calcite vein; C.S.: Crack-seal vein; S.V.: Satellite vein; St.: Stylolite; Br.: Breccia; Cav.: Cavity. So: Bedding.

Fig. 7: (a) Complex zone of shearing in Espréaux showing angular fragments of calcite veins in a clay-rich matrix. (a) General view. (b) Detail view. (c) Model for the formation of the microstructures in (a) with imbrication. Shear movement of the clay in a shear zone generates failure, imbrication and rotation of the calcite vein fragments. (d) Alternative model for the formation of the microstructures in (a) with rotations and fragmentation of the BPF. (e) Examples of complex microstructures observed at Espréaux. (f) Detail of echelon fuzzy structures and crack-seals. (a-f) C.V.: Calcite vein; Cl.: Wall rock; C.S.: Crack-seal vein; S.V.: Satellite vein; St.: Stylolite; S.Z.: shear zone; F.V.:Fuzzy vein. So: Bedding.

Fig. 8: Models for bedding-parallel fault history. In model 1, bedding-parralel faults (BPFs) are monophased and all microstructures formed during the same tectonic event. In models 2 and 3, BPFs are polyphase structures and were active during successive deformational events of the basin. In model 2, BPFs first slipped during the Oligocene extensional tectonics and were later reactivated during the alpine inversion. In model 3, the BPFs initiated as opening fracture and were reactivated during all subsequent tectonic events. Time uncertainrty for opening and pressure solution is indicated by grey arrow. Each model reflects the successive movements along the BPFs deduced from microstructures and outcrop observations: shearing (blue during extensional tectonics and red during compressional tectonics) and opening normal to bedding. See text for more details and mechanical implication. Model 1 does not apply for the studied BPFs (expect eventually in Saint-Didier site), but may represent other example of BPFs. Exemples from this study support a long-lived history of BPFs.

Fig. 9: Cartoons illustrating two potential contexts of formation of bedding-parralel faults (BPFs). (a) A segmented BPF formed due to flexural slip mechanism to accommodate bed-parallel slip. Slip is partitioned along different segments of the BPF and normal faults occur in the releasing steps (e.g., *Pedrera et al., 2012; Delogkos et al., 2018*). Arrows: shear sense. (b) Bi-modal faulting in multilayer

649 rocks. Failure follows the Andersonian mode in the limestones (high dipping normal faults are
650 formed) whereas it does not in the clays (BFPs are formed). These two types of faults later propagate
651 and connect each other. Convergent and divergente arrows: compression and extension.
652

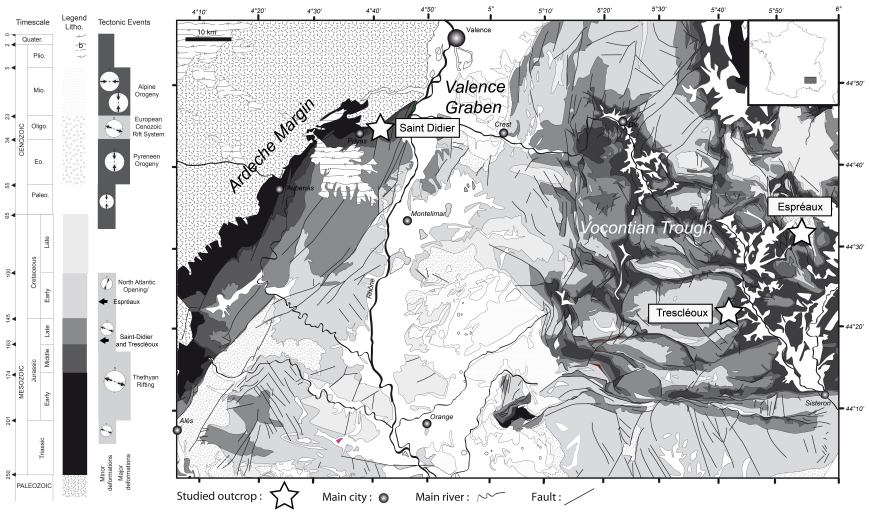

(a) Trescléoux

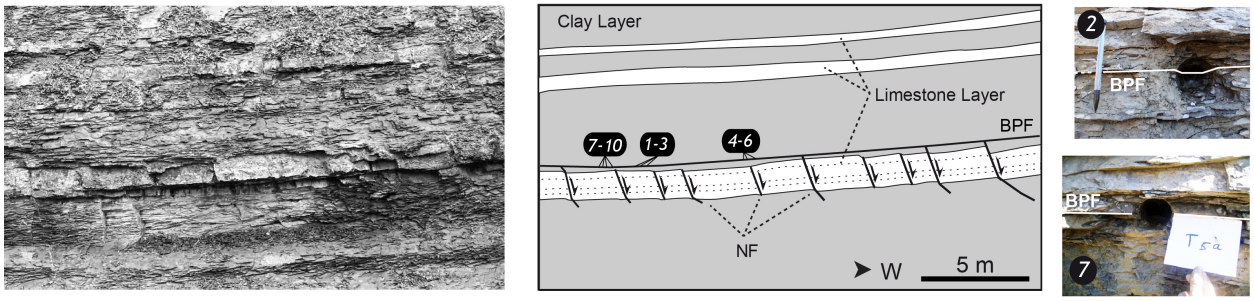

(b) Espréaux

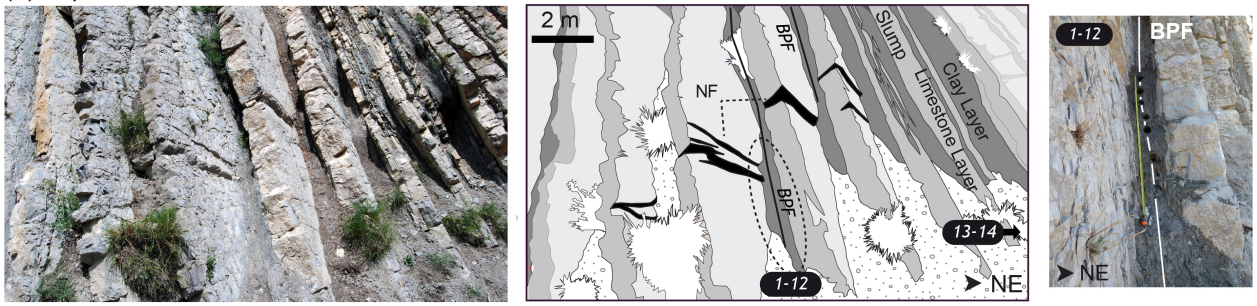

(c) Saint-Didier

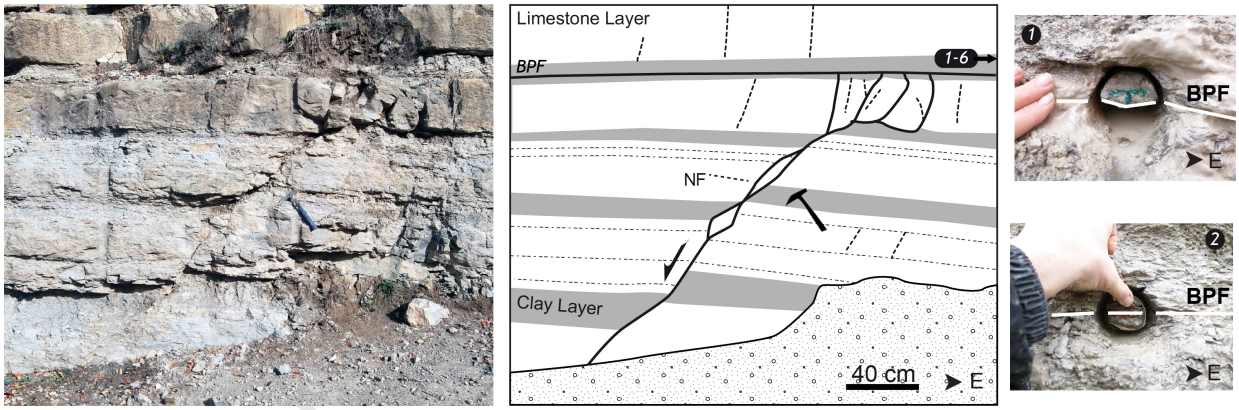

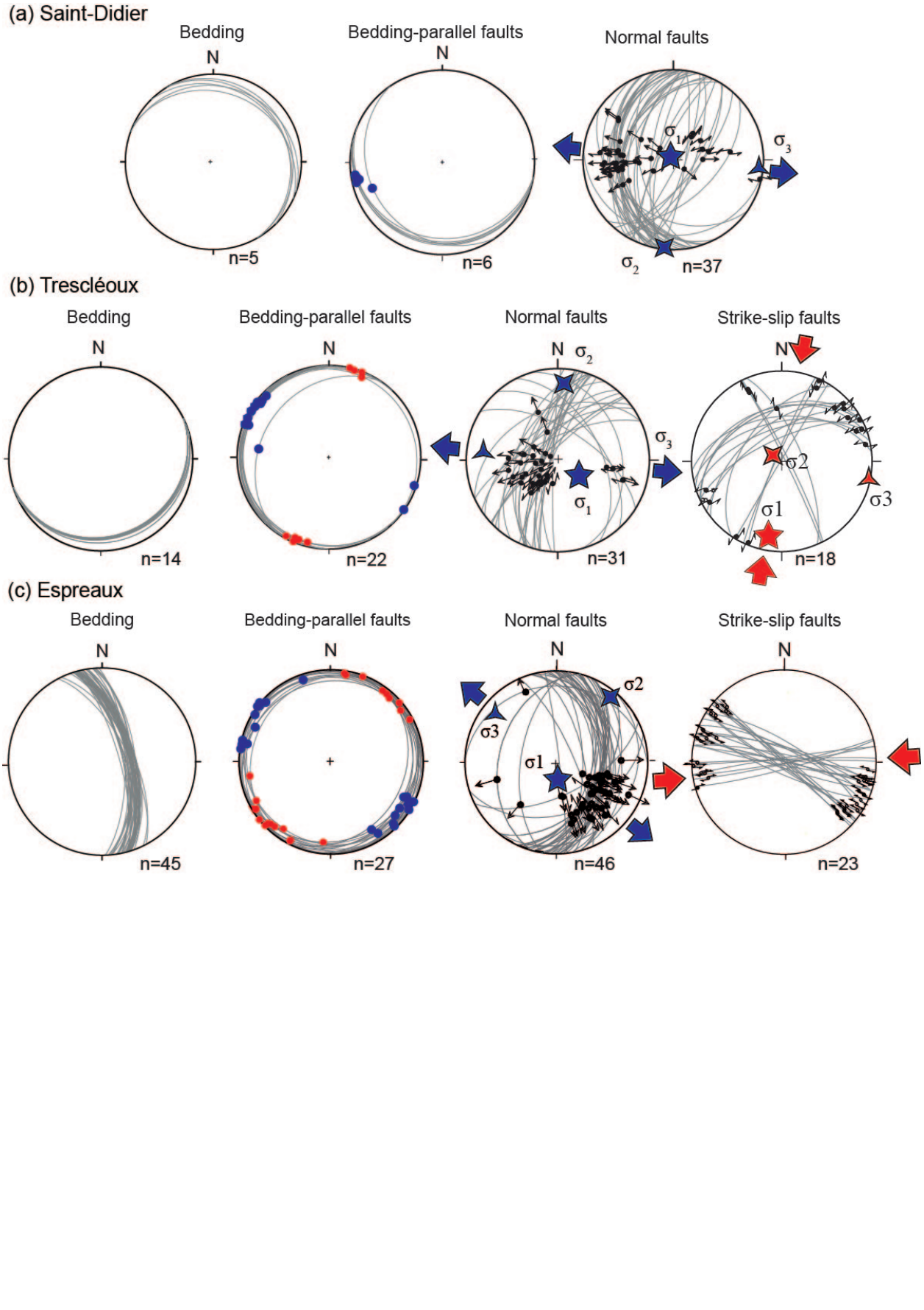
(a) Saint-Didier
Bedding
Bedding-parallel faults
Normal faults
N
N
N
σ1
σ3
σ2
n=5
n=6
n=37
(b) Trescléoux
Bedding
Bedding-parallel faults
Normal faults
Strike-slip faults
N
N
N
σ2
N
σ3
σ2
σ1
σ3
σ1
n=14
n=22
n=31
n=18
(c) Espreaux
Bedding
Bedding-parallel faults
Normal faults
Strike-slip faults
N
N
N
N
σ2
σ3
σ1
n=45
n=27
n=46
n=23

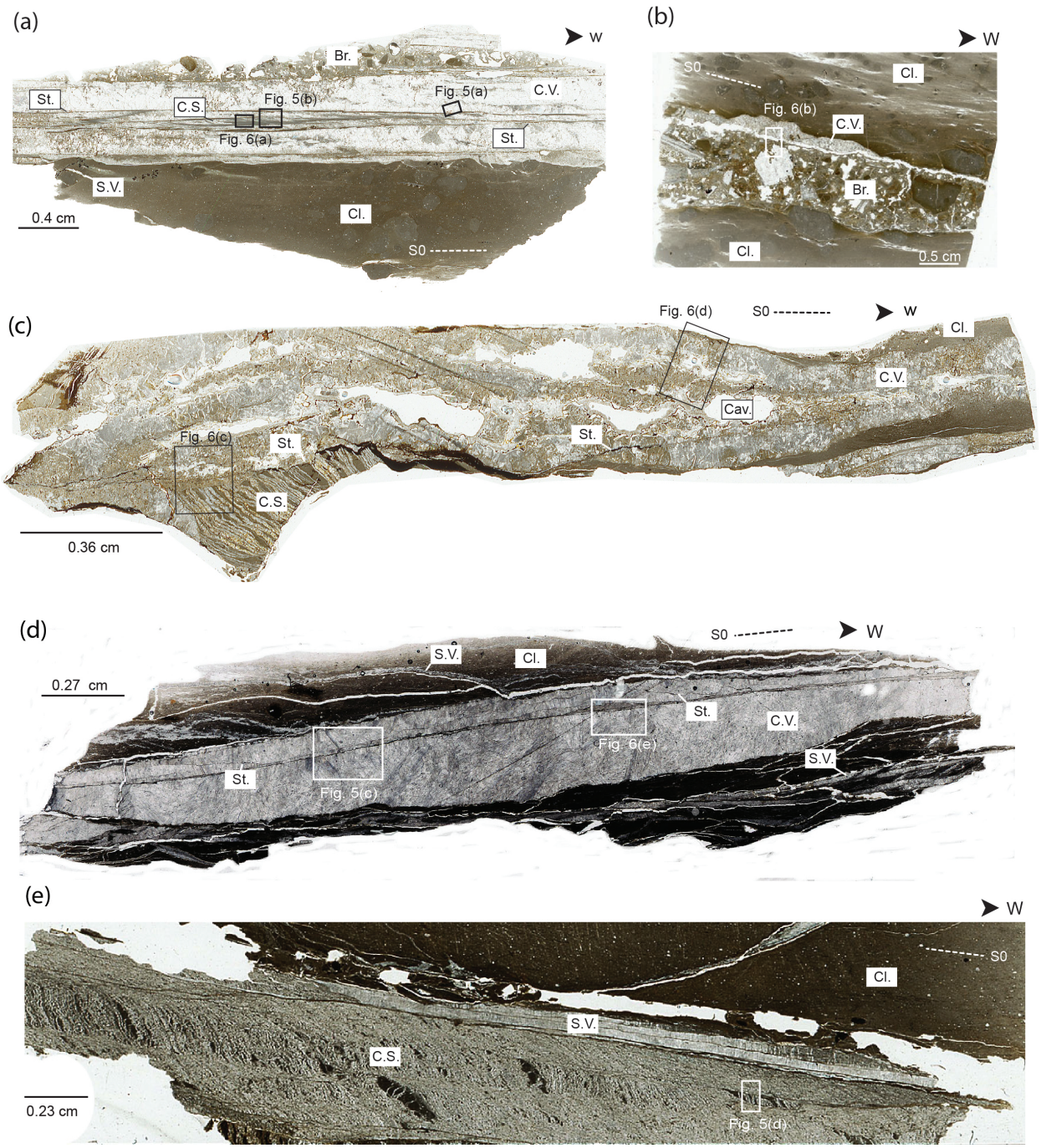
(a)
W
Br.
St.
C.S.
Fig. 5(b)
Fig. 5(a)
C.V.
Fig. 6(a)
St.
S.V.
0.4 cm
Cl.
S0
(b)
W
S0
Cl.
Fig. 6(b)
C.V.
Br.
Cl.
0.5 cm
(c)
Fig. 6(d)
S0
W
Cl.
C.V.
Cav.
Fig. 6(c)
St.
St.
C.S.
0.36 cm
(d)
S0
W
S.V.
Cl.
0.27 cm
St.
C.V.
Fig. 6(e)
S.V.
St.
Fig. 5(c)
(e)
W
S0
Cl.
S.V.
C.S.
0.23 cm
Fig. 5(d)

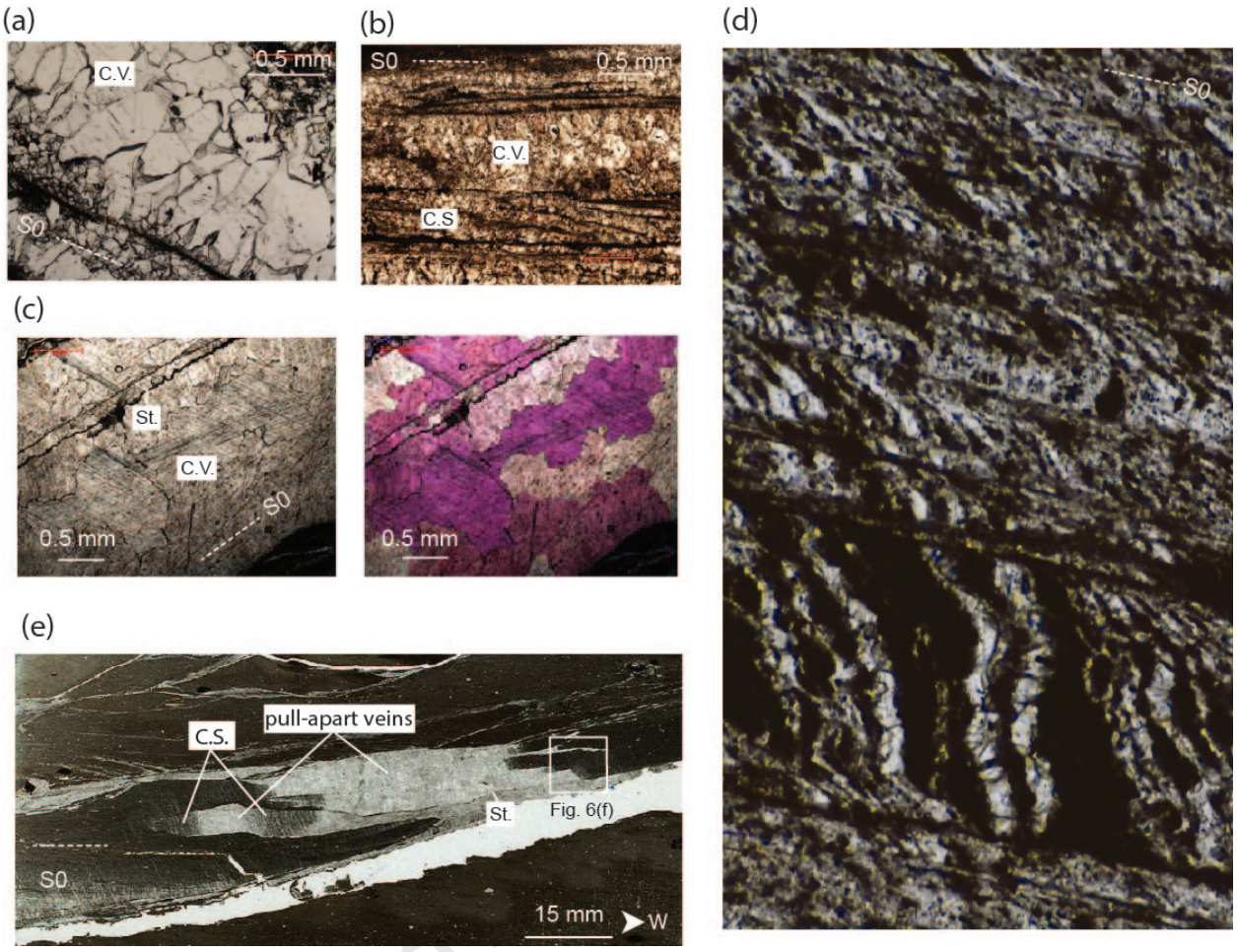
(a)
C.V.
0.5 mm
S0
(b)
S0
0.5 mm
C.V.
C.S
(c)
St.
C.V.
S0
0.5 mm
0.5 mm
(d)
S0
(e)
C.S.
pull-apart veins
St.
Fig. 6(f)
S0
15 mm
W

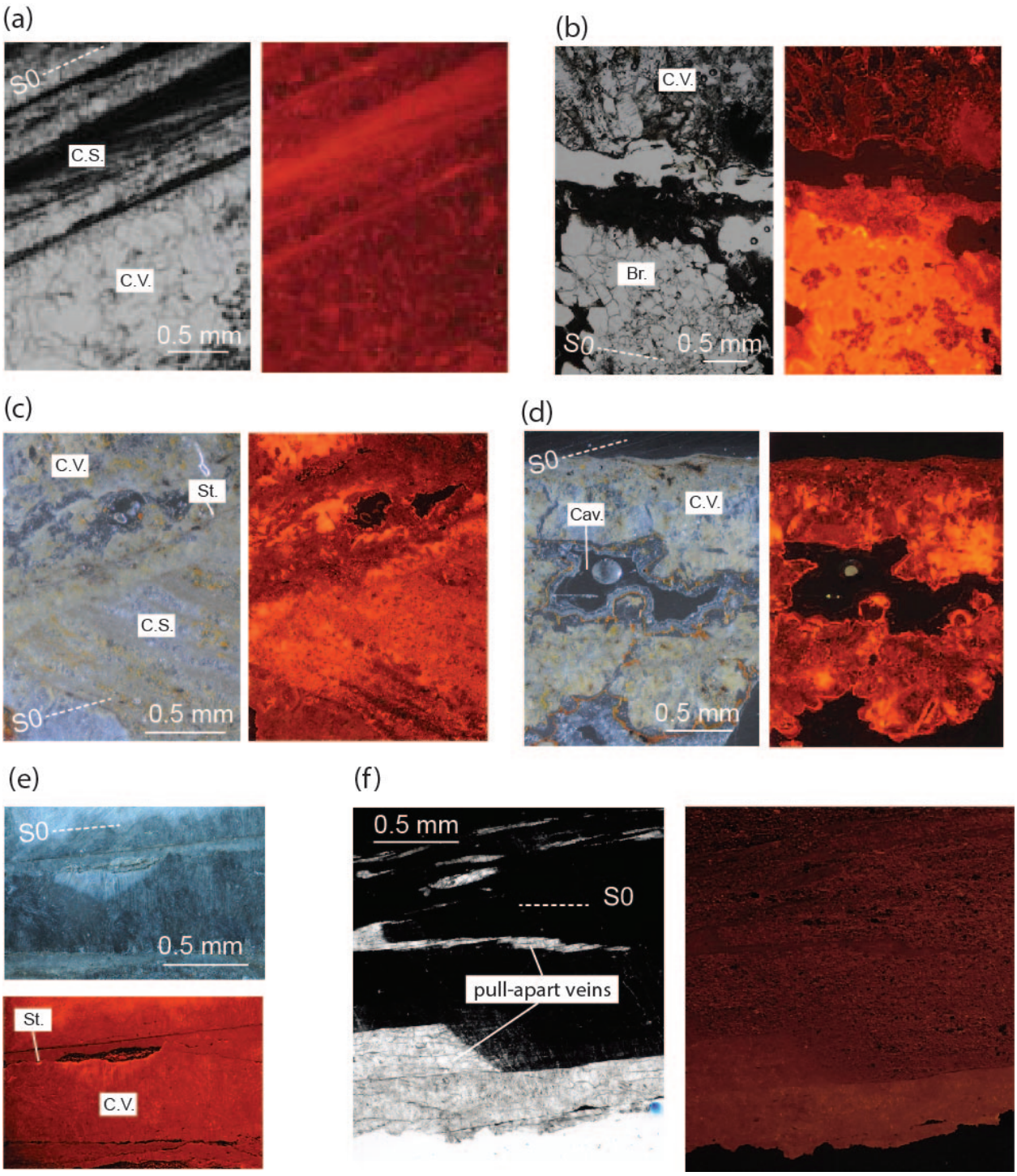
(a)
S0
C.S.
C.V.
0.5 mm
(b)
C.V.
Br.
S0
0.5 mm
(c)
C.V.
St.
C.S.
S0
0.5 mm
(d)
S0
Cav.
C.V.
0.5 mm
(e)
S0
0.5 mm
St.
C.V.
(f)
0.5 mm
S0
pull-apart veins

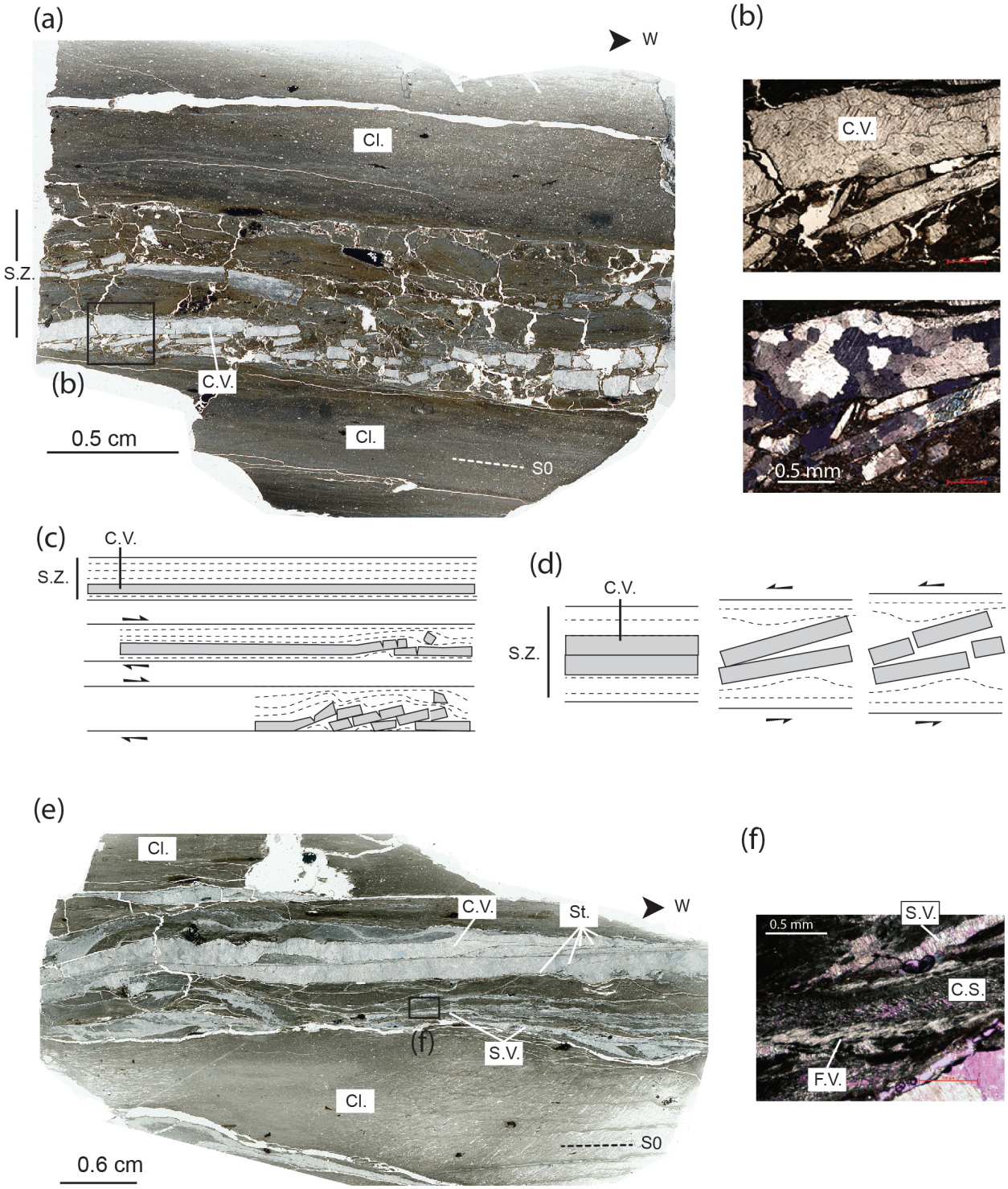
(a)
W
Cl.
S.Z.
(b)
C.V.
Cl.
S0
0.5 cm
(b)
C.V.
C.V.
0.5 mm
(c)
C.V.
S.Z.
(d)
C.V.
S.Z.
(e)
Cl.
C.V.
St.
W
(f)
S.V.
Cl.
S0
0.6 cm
(f)
0.5 mm
S.V.
C.S.
F.V.

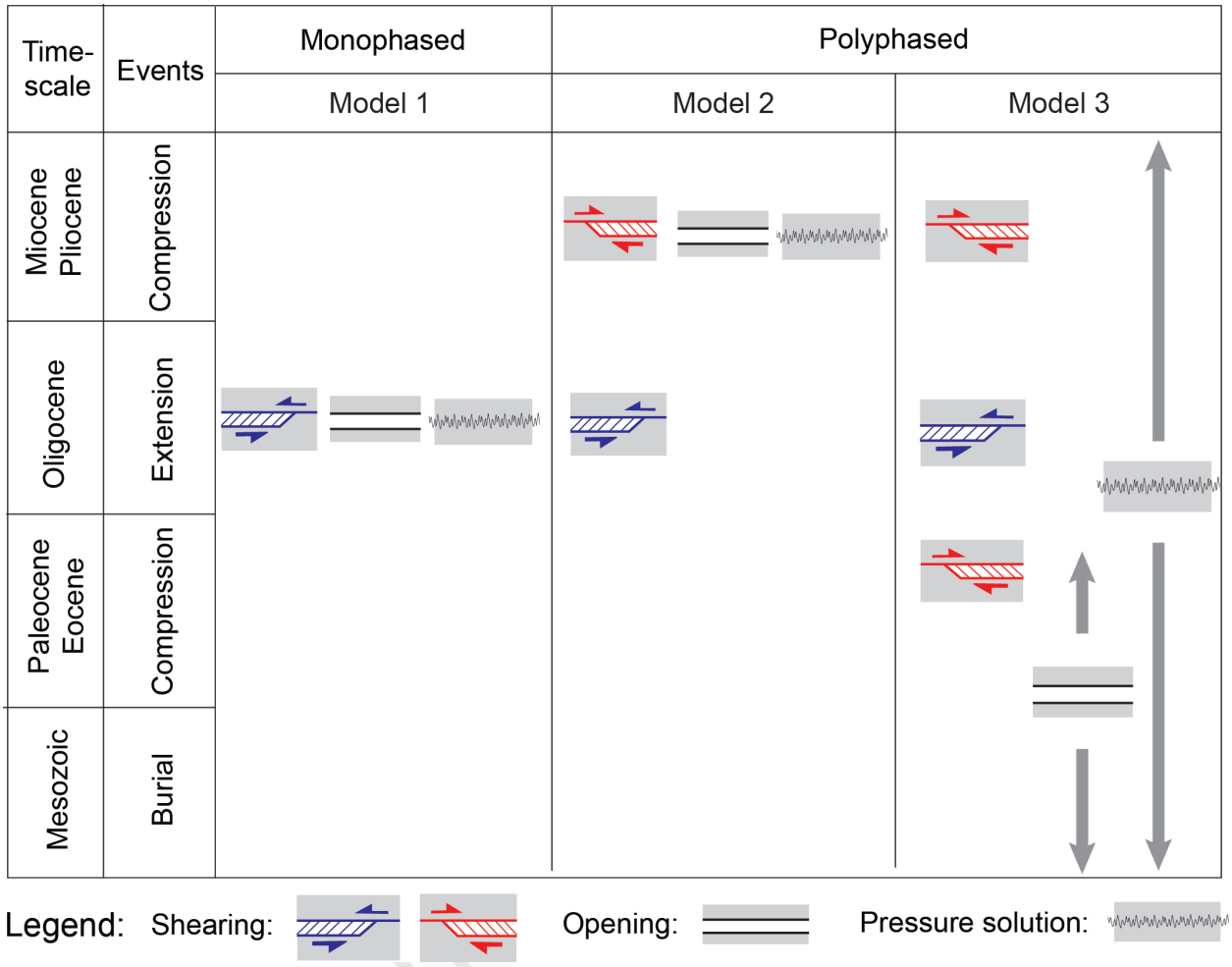
Time-scale
Events
Monophased
Polyphased
Model 1
Model 2
Model 3
Miocene Pliocene
Compression
Oligocene
Extension
Paleocene Eocene
Compression
Mesozoic
Burial
Legend:
Shearing:
Opening:
Pressure solution:

(a)

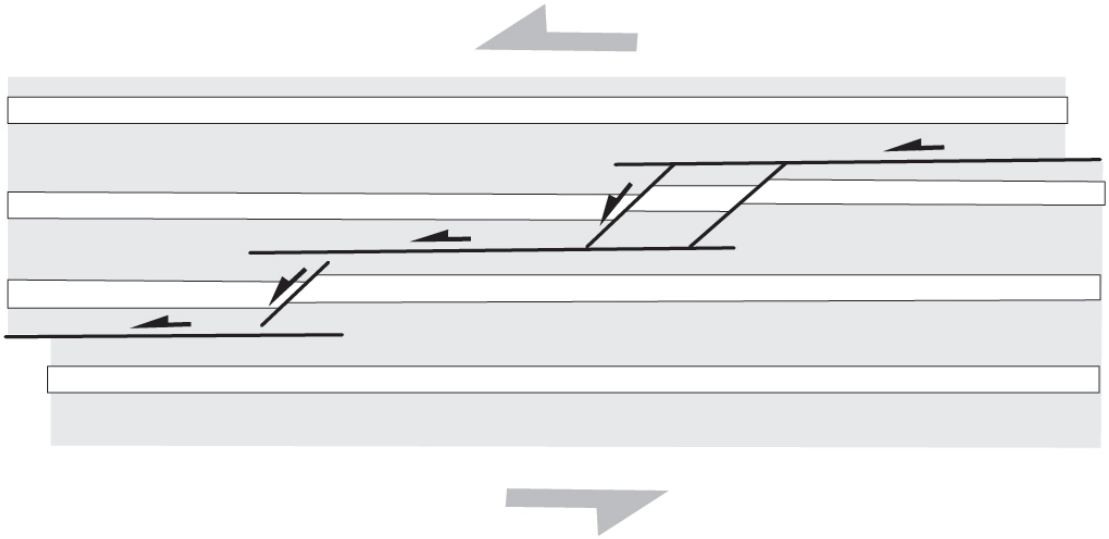

(b)

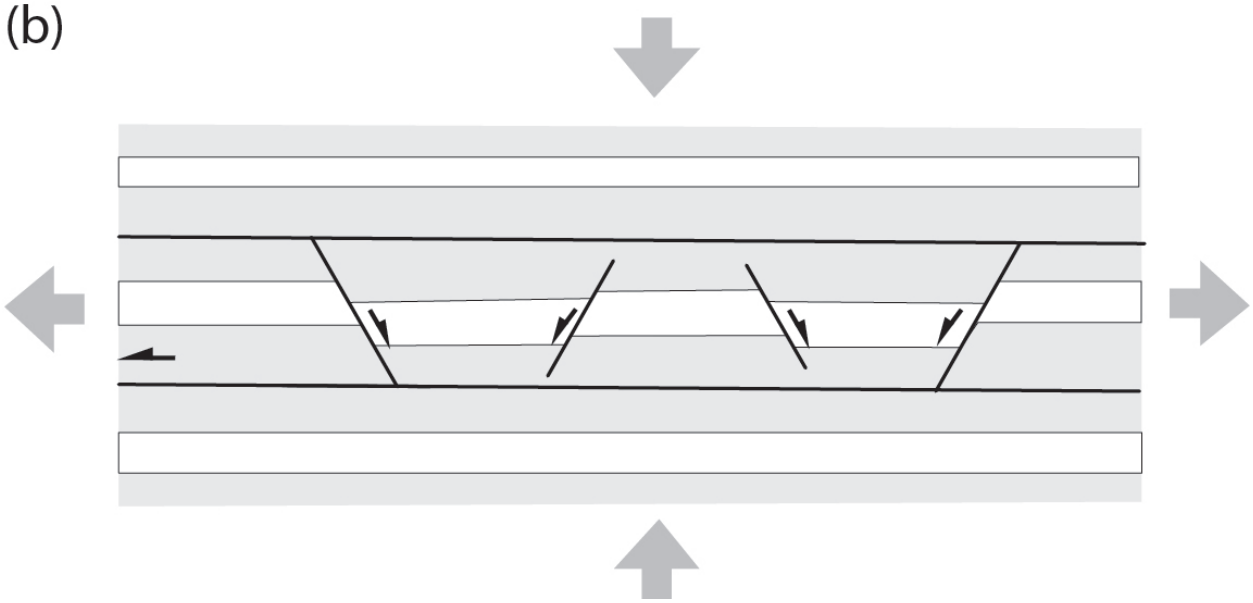

ISTeP Institut des Sciences de la Terre de Paris
UMR 7193-UPMC-CNRS

UPMC SORBONNE UNIVERSITÉS
cnrs INSU Observer & comprendre

Paris, 6th July 2020

Ref: SG_2019_403
Journal: Journal of Structural Geology

The authors declare that they have no known competing financial interests or personal relationships that could have appeared to influence the work reported in this paper.

They have seen and approved the final version of the manuscript being submitted. They warrant that the article is the *authors*' original work, hasn't received prior publication and isn't under consideration for publication elsewhere.

Sincerely, Catherine Homberg

Institut des Sciences de la Terre Paris – ISTeP
UMR 7193 CNRS-UPMC
4 place Jussieu - Case 129 - 75252 Paris Cedex 05

catherine.homberg@sorbonne-universite.fr
Tél. 33-1 44 27 52 74
www.istep.upmc.fr